The Journal of Infectious Diseases

MAJOR ARTICLE

Central Role for Dermal Fibroblasts in Skin Model Protection against Candida albicans

Andreas Kühbacher,[1] Helena Henkel,[1] Philip Stevens,[1,3] Christian Grumaz,[1] Doris Finkelmeier,[1] Anke Burger-Kentischer,[1,2] Kai Sohn,[1,2] and Steffen Rupp[1,2]

[1]Department of Molecular Biotechnology, Fraunhofer Institute for Interfacial Engineering and Biotechnology, and [2]Institute of Interfacial Process Engineering and Plasma Technology, University of Stuttgart, Germany; and [3]Center for Integrative Bioinformatics Vienna, Max F. Perutz Laboratories, University of Vienna, Medical University of Vienna, Austria

The fungal pathogen *Candida albicans* colonizes basically all human epithelial surfaces, including the skin. Under certain conditions, such as immunosuppression, invasion of the epithelia occurs. Not much is known about defense mechanisms against *C. albicans* in subepithelial layers such as the dermis. Using immune cell–supplemented 3D skin models we defined a new role for fibroblasts in the dermis and identified a minimal set of cell types for skin protection against *C. albicans* invasion. Dual RNA sequencing of individual host cell populations and *C. albicans* revealed that dermal invasion is directly impeded by dermal fibroblasts. They are able to integrate signals from the pathogen and $CD4^+$ T cells and shift toward an antimicrobial phenotype with broad specificity that is dependent on Toll-like receptor 2 and interleukin 1β. These results highlight a central function of dermal fibroblasts for skin protection, opening new possibilities for treatment of infectious diseases.

Keywords. *Candida albicans*; dermal fibroblasts; $CD4^+$ T cells; Toll-like receptor 2 (TLR2); interleukin 1β (IL-1β).

As a commensal pathogen, *Candida albicans* colonizes human epithelial surfaces such as the oral and vaginal mucosa, the intestine, and the skin, usually without causing disease. Temporary superficial infections of the vaginal mucosa is common and experienced at least once by up to 75% of women [1]. Moreover, under conditions of immunosuppression, patients suffer from recurrent infections at multiple sites [2–5], highlighting the requirement of a functional immune system for keeping *C. albicans* in a nonpathogenic state. Traversal of epithelial barriers is a critical process of pathogenesis because it may grant the fungus access to the blood stream. The barrier function of epithelial surfaces is, therefore, essential for protection against systemic candidiasis. It has been shown that this barrier function against *C. albicans* invasion is dependent on various cell types and involves cross-talk between epithelial cells, neutrophil granulocytes, Th17 cells, and γδ T cells and varies between different sites of infection [2, 6–8]. Keratinocytes can directly react to *C. albicans* with Toll-like receptor 2 (TLR2)–dependent expression of antimicrobial peptides such as β-defensins and LL-37 [9]. Moreover, upon release of inflammatory mediators by epithelial cells, neutrophils are recruited early to the site of fungal penetration where they promote fungal killing, directly and indirectly [10]. For example, it was shown that neutrophils induce upregulation of the pattern recognition receptor (PRR) Toll-like receptor 4 in oral epithelial cells through tumor necrosis factor α (TNFα), potentiating fungal recognition and tissue protection [6]. On the other hand, Th17 cells were shown to protect oral epithelial cells against *C. albicans* invasion independently of neutrophils. Secretion of interleukin 17 (IL-17) by these cells leads to the induction of antimicrobial peptides and fungal clearance [7]. If the epithelial barrier is breached, access of the pathogen to the blood stream may in principle be granted in the subepithelial tissue. Nevertheless, although *C. albicans* colonizes human skin as a commensal organism, systemic dissemination does not normally originate from skin barrier crossing, even in immunocompromised individuals with recurrent mucocutaneous candidiasis [11, 12]. This highlights that efficient defense mechanisms at the level of the dermis may account for pathogen clearance. Such mechanisms are, however, currently not well described. It has been shown that $CD301b^+$ dermal dendritic cells recognize *C. albicans* in subepithelial tissue and induce a Th1 response, which also involves macrophages, that is protective against systemic infection [2, 5, 13]. We show that, in addition to keratinocytes and immune cells, dermal fibroblasts play a critical role in antimicrobial defense.

Received 30 November 2016; editorial decision 17 March 2017; accepted 23 March 2017; published online March 29, 2017.

Presented in part: 13th ASM Conference on Candida and Candidiasis, Seattle, Washington, 13–17 April 2016. Abstract S8A:3. 5th Joint Microbiology and Infection Conference of the Deutsche Gesellschaft für Hygiene und Mikrobiologie (DGHM) & Vereinigung für Allgemeine und Angewandte Mikrobiologie (VAAM), Würzburg, Germany, 5–8 March 2017. Abstract 235/IIV.

Correspondence: S. Rupp, Dr. rer. nat., Nobelstr 12, 70569 Stuttgart, Germany (steffen.rupp@igb.fraunhofer.de).

The Journal of Infectious Diseases® 2017;215:1742–52

DOI: 10.1093/infdis/jix153

METHODS

Cell Culture and Fungi

S1F immortalized human dermal fibroblasts were obtained from the Rheinwald laboratory [14, 15]. Immortalized *Irak4*-deficient human dermal fibroblasts (patient 2336) were

provided by Anne Puel [16]. Ker-CT immortalized human keratinocytes were obtained from American Type Culture Collection [17]. NIH3T3-SEAP-TLR2/1 and NIH3T3-SEAP-TLR2/6 were described previously [18]. Naive $CD4^+$ T cells were isolated by negative selection from peripheral blood mononuclear cells (PBMCs) purified from buffy coat from voluntary male donors. Informed consent was given by donors of human blood. For infections, *C. albicans* strain SC5314 [19] was used. See the Supplementary Methods for additional information.

3D Tissue Culture

The 3D skin equivalents were grown by first seeding fibroblasts in a collagen matrix in trans-well cell-culture inserts and subsequently seeding keratinocytes on top [20]. After 10 days of culture at the air–liquid interface, PBMCs or $CD4^+$ T cells were embedded in collagen and placed underneath the tissue model. See the Supplementary Methods for additional information.

Infection of 3D Skin Models

Skin models were infected with 100 colony-forming units of a *C. albicans* culture overnight. For RNA sequencing, cell layers were separated 24 hours after infection and frozen down in liquid nitrogen. For histology and infection quantification, samples were fixed in Bouins solution for 12 hours–6 days after infection. See the Supplementary Methods for additional information.

Histology and Immunohistochemistry

For histological analysis and immunostaining, 3-μm tissue sections were prepared and deparaffinized. Sections were stained with Mayer's Hemalaum (Merck) for 8 minutes and Eosin (Fluka) for 1 minute according to a standard HE procedure. *Candida albicans* was visualized by a periodic acid Schiff (PAS) staining procedure as described previously [21]. See the Supplementary Methods for additional information.

Invasion Quantification

Candida albicans dermal invasion was quantified by measuring the infected dermal area and the total dermal area of HE- or periodic acid Schiff–stained tissue sections using ImageJ [22]. Depth of dermal invasion was then calculated as the ratio of infected and total area and shown as box plots indicating the median and the 25% and 75% quartiles of several images of up to 3 individual models. Individual data points representing each image are additionally shown as dots. Red green and blue dot colors refer to the model from which the image originates. For statistical analysis, the 2-tailed Wilcoxon-Mann-Whitney *U* test was used. This readout was validated with models treated with 4 μg/mL of the antifungal fluconazole to block invasion at different time points.

RNA Sequencing and Analysis of Sequencing Data

For differential gene expression analysis, total RNA was isolated from individual host-cell populations of skin models and *C. albicans*. mRNA was isolated and library preparation was done using the TruSeq RNA Sample Preparation Kit v2 (Illumina). All sequencing experiments were done with 3 independent tissue models per group. Sets of differentially expressed genes (false discovery rate < 0.05) were functionally analyzed by Ingenuity pathway analysis (IPA) for human genes and by GO term enrichment analysis for *C. albicans* genes.

The raw data discussed in this article have been deposited in the National Center for Biotechnology Information's Gene Expression Omnibus [23] and are accessible through GEO Series accession number GSE86926 (https://www.ncbi.nlm.nih.gov/geo/query/acc.cgi?acc=GSE86926). See the Supplementary Methods for additional information.

Pathogen-associated Molecular Pattern Assay

The principle of the NF-κB reporter gene assay has been described previously [18]. It relies on photometric activity measurement of the reporter gene–secreted alkaline phosphatase (SEAP) in the cell-culture supernatant of human skin models or cells grown in a 96-well plate format. See the Supplementary Methods for additional information.

Western Blot

Expression of interleukin 1β (IL-1β) was detected by Western blot using the iBlot 2 system and a rabbit-derived primary antibody (1030A5.138; Novus). See the Supplementary Methods for additional information.

Enzyme-Linked Immunosorbent Assay

Interleukin 1β, CXCL9, CXCL10, and CXCL11 in cell-culture medium was measured by enzyme-linked immunosorbent assay (ELISA). See the Supplementary Methods for additional information.

Caspase-1 Activity Assay

Caspase-1 activity in cell culture supernatants was measured using the Caspase-Glo 1 Inflammasome Assay (Promeg). See the Supplementary Methods for additional information.

RESULTS

Response of Keratinocytes and Fibroblasts to *Candida albicans* Invasion

To identify the minimal requirements for dermal protection against *C. albicans*, we used several variants of 3D tissue models of the skin. Interestingly, we could generate a skin model significantly protected against *Candida* invasion using only 3 cell types: human keratinocytes, dermal fibroblasts embedded in a collagen matrix (Supplementary Figure 1A and 1B), and component $CD4^+$ T cells. In contrast with what is known for natural human skin, models containing only dermal fibroblasts and keratinocytes are highly permissive to deep *C. albicans*

invasion (Supplementary Figure 1C). Transcriptional profiling of infected and uninfected 3D tissue models containing only fibroblasts and keratinocytes revealed, after separation of epidermal and dermal compartments (Supplementary Figure 1D), that keratinocytes react strongly to *C. albicans* infection, with upregulation of 70 genes (Figure 1A; Supplementary Figure 1E; Supplementary Table 1). However, this is not sufficient to block invasion. In fibroblasts, expression of only 18 genes, most of which were predicted by IPA to be regulated by the transcription factor AP-1, were significantly induced with a log fold change of at least 1.5 (Figure 1A; Supplementary Figure 1F; Supplementary Table 1). In keratinocytes and fibroblasts, only 2 and 3 genes, respectively, were downregulated upon infection. As predicted by IPA, transcriptional changes in both cell types were predominantly related to an inflammatory response and chemotaxis of immune cells (Figure 1B and 1C). Whereas in keratinocytes, for example, the metal ion–sequestering antimicrobial peptides S100A8 and S100A9 were strongly expressed already in steady-state conditions, there was no indication of a direct fibroblast-derived defense response that may restrict

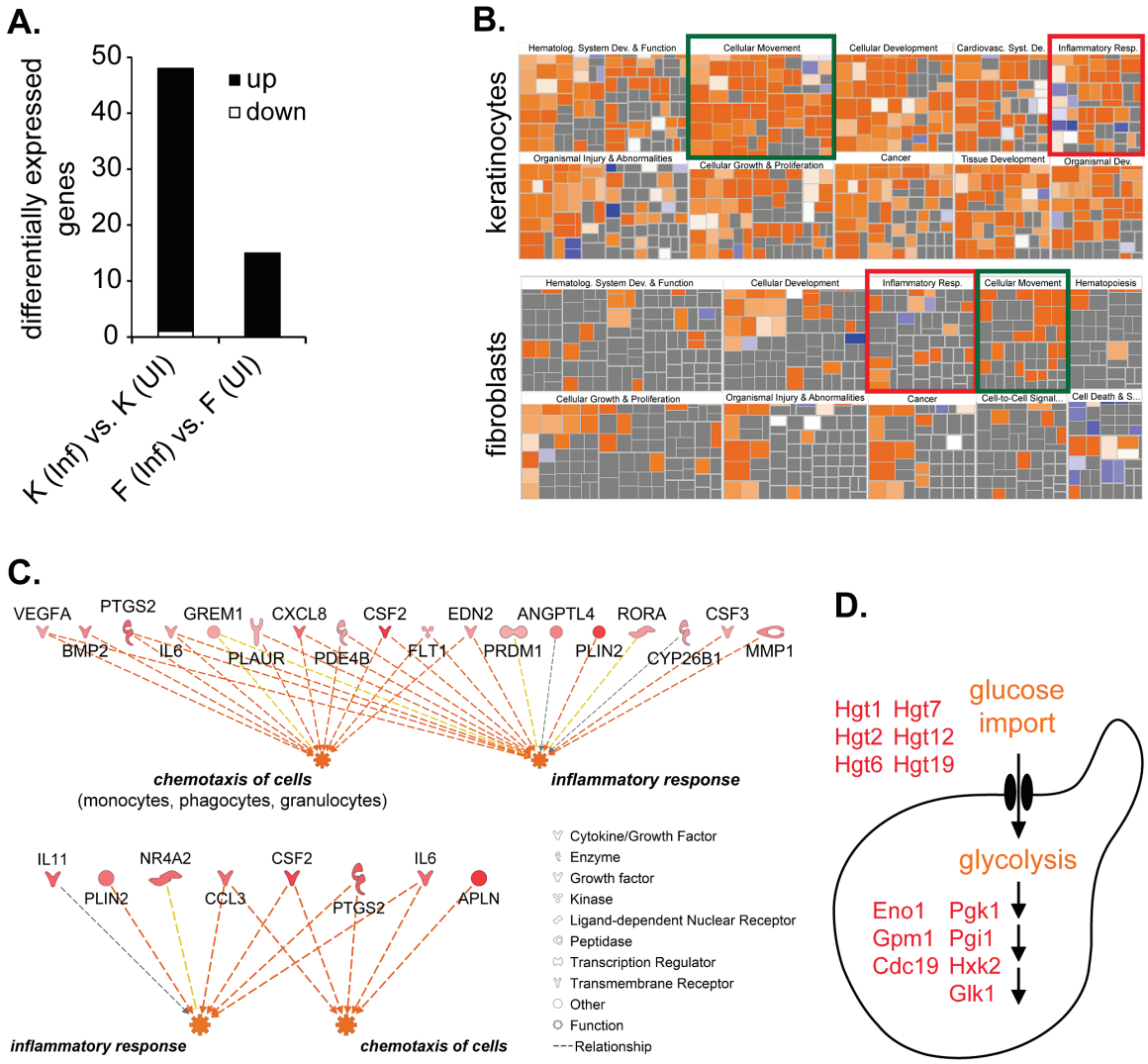

Figure 1. Differential expression analysis of keratinocytes, fibroblasts, and *Candida albicans* during skin model invasion. Human skin models containing dermal fibroblasts embedded in a collagen matrix and keratinocytes were kept uninfected or infected with *C. albicans* yeast cells. After 24 hours, epidermis and dermis were separated mechanically and processed for RNA sequencing. *A,* Number of up- (black bars) and downregulated (white bars) genes in keratinocytes and fibroblasts upon infection. *B,* Ingenuity pathway analysis (IPA) of differentially expressed genes (DEGs) in keratinocytes and fibroblasts. Heat maps show the *z* score (2 = orange and –2 = blue) of up- and downregulated cellular functions and diseases in the presence of $CD4^+$ T cells, predicted based on expressional changes. Threshold in *A* and *B*: average log2 fold change (log2FC) of biological triplicates < –1.5 or > 1.5. Functions related to cellular movement and to an inflammatory response are highlighted by a green and red box, respectively. *C,* Networks of DEGs after infection from keratinocytes (upper panel) and fibroblasts (lower panel) resulting in selected diseases and functions based on IPA. Upregulated genes are colored in red and predicted upregulated functions in orange. Orange lines indicate consistent and yellow lines inconsistent connections. Gray lines show connections with unpredictable outcome. *D,* Differential expression analysis of *C. albicans* genes. Significantly upregulated functions in the dermis compared with the epidermis based on GO-term enrichment analysis are colored in orang,m and upregulated genes belonging to these functions are shown in red. Thresholds: log2FC < –1 or > 1, log2CPM > 2.5. Abbreviations: F, fibroblast; GO, gene ontology; Inf, infected; K, keratinocytes; UI, uninfected.

fungal invasion (Supplementary Figure 1G). Differential expression analysis of fungal genes in dermal and epidermal compartments (Supplementary Figure 1H) further revealed that, once in the dermis, *C. albicans* downregulates genes involved in a stress response, such as the glucose-6-phosphate dehydrogenase *ZWF1*, and nutrient and metal ion restriction, including *ZRT1* and *PRA1,* which were recently shown to act together in zinc sequestration [24]. In contrast, genes related to glucose transport and glycolysis, such as *HGTs 1, 2, 6, 7, 12, and 19* and *HXK2,* are induced, further indicating that the pathogen does not encounter a defense response in the dermal part of this 2-component skin model (Figure 1D; Supplementary Table 2).

Antimicrobial Response of Fibroblasts in the Presence of CD4⁺ T Cells and *Candida albicans*

Several genes upregulated in keratinocytes and fibroblasts upon infection were related to attraction and differentiation of immune cell subsets, including CD4⁺ T cells (Figure 2A). To analyze the effect of attracted immune cells, we tested for a role of blood components in dermal protection against *C. albicans* invasion. Indeed, whole blood provided basolaterally to the tissue culture medium significantly reduced dermal invasion. The same effect could be observed by integration of isolated PBMCs in a gel-layer placed below the dermal layer (basolaterally) (Figure 2B). For more robust analysis of this phenotype, we developed a readout for the depth of invasion based on image quantification (Supplementary Figure 2*A*), which confirmed a significant reduction of *C. albicans* invasion in the presence of human blood or PBMCs (Figure 2C). Efficient protection was already achieved by adding only CD4⁺ T cells isolated from human blood and activated before integration (Figure 2D). Interestingly, we could show that keratinocytes were dispensable for the protective effect observed (Supplementary Figure 2B). Therefore we concluded that fibroblasts may be directly involved in this process. Indeed transcription profiles of fibroblasts from infected skin models changed drastically in the presence of CD4⁺ T cells, with 256 genes being significantly induced and 38 genes downregulated at a log fold change of at least 1.5 (Supplementary Figure 2C and 2D; Supplemetnary Table 3). Analysis of single nucleotide polymorphisms (SNPs) in mitochondrial sequences and selected genomic regions showed that cross-contamination of fibroblasts with keratinocyte- or T cell–derived RNA was minor or absent, respectively (Supplementary Figure 2E). Further analysis of the differential

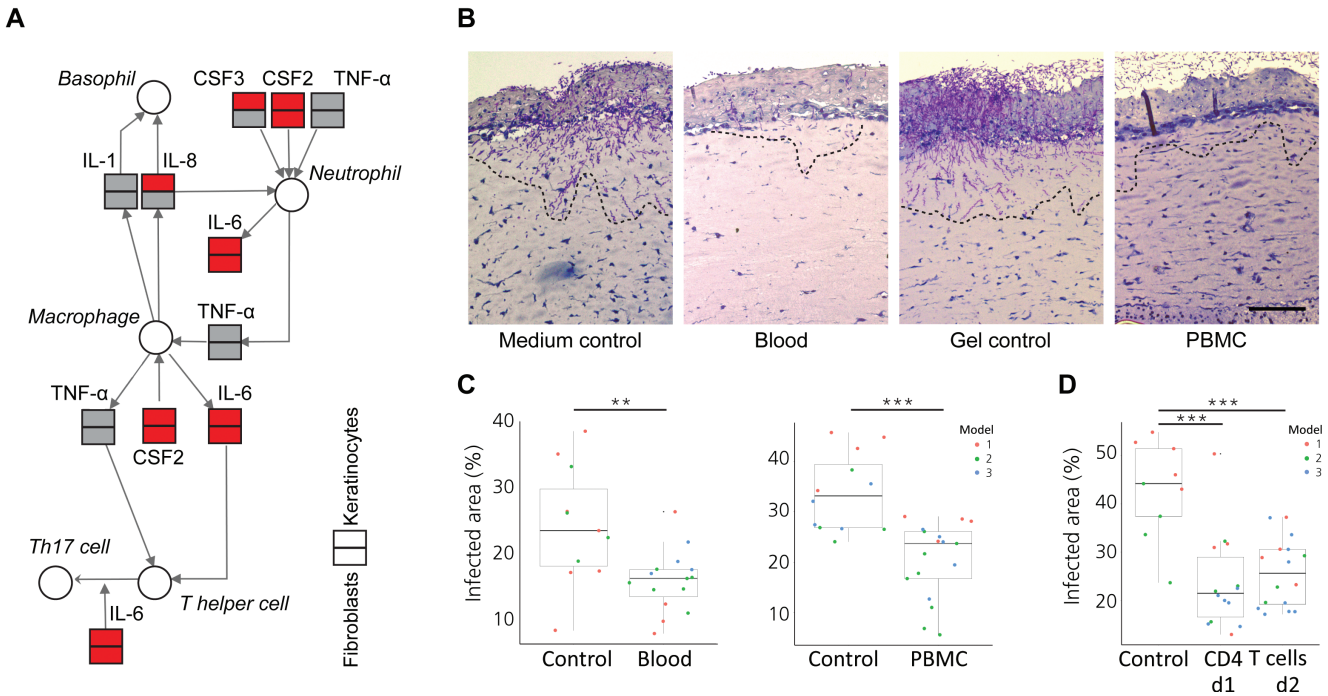

Figure 2. Influence of blood cells on *Candida albicans* infection of skin models. *A*, Upregulated cytokines and chemokines in keratinocytes and fibroblasts upon skin model infection mapped by Ingenuity pathway analysis to the canonical pathway of immune-cell trafficking and differentiation. Red boxes show upregulated genes, and gray boxes show genes not differentially expressed. *B*, Periodic acid Schiff–stained sections of human skin models consisting only of keratinocytes and fibroblasts or supplemented with whole blood or isolated peripheral blood mononuclear cells and infected with *C. albicans* for 24 hours. The border of *C. albicans* invasion into the dermis is indicated by a dotted line. Bar: 100 µm. *C*, Image quantification of the depth of dermal invasion by *C. albicans* 24 hours after infection. *D*, Quantification of *C. albicans* dermal invasion of skin models 48 h after infection with or without CD4⁺ T cells from 2 different donors. Significant differences (2-tailed Wilcoxon-Mann-Whitney *U* test) in *C* and *D* are indicated by ** ($P < .01$) and *** ($P < .001$). Abbreviations: IL-1, interleukin 1; IL-6, interleukin 6; IL-8, interleukin 8; PBMC, peripheral blood mononuclear cell; TNFα, tumor necrosis factor α.

expression profiles by IPA revealed that this transcriptional reprogramming of dermal fibroblasts resulted not only in general upregulation of innate immune mechanisms such as inflammation but also in a direct antimicrobial response (Figure 3A and 3B). Among the strongest upregulated genes were the 3 chemokines *CXCL9*, *CXCL10*, and *CXCL11* (Figure 3B), which were shown previously to exert direct antimicrobial activity [25]. Upregulation of these chemokines was confirmed by ELISA (Figure 3C). Interestingly, particularly for CXCL10, which was the highest expressed, direct activity against *C. albicans* has been shown [26]. Even though the precise nature of chemokine antimicrobial activity is not known, there may be similarities to β-defensins [25, 27], some of which—namely HBD1, 2, and 3—are known antifungal peptides [28, 29]. Moreover, we could observe strong upregulation of the guanylate binding protein *GBP2*, which is involved in killing of the bacterial pathogens *Chlamydia trachomatis* and *Francisella novicida* and the parasite *Toxoplasma gondii* by different mechanisms [30–32], as well as a set of interferon-stimulated antiviral genes, including *OAS1*, *MX1*, *MX2* and *ISG15* (Figure 3B). Hence, the fibroblast-derived antimicrobial response was not specific to fungal infection but targeted toward a broad spectrum of pathogens (Figure 3B).

The dual RNA-sequencing approach allowed us to analyze the fungal reaction to the fibroblast response in the presence of CD4⁺ T cells. *Candida albicans* in the dermis of T cell–supplemented skin models showed significant overexpression of genes related to changes in metabolism, including an upregulation of *SIT1* and *CFL1*, which are involved in iron capturing, and the glyoxylate cycle–related genes *ICL1* and *MLS1* (Figure 3D; Supplementary Figure 2F; Supplementary Table 4). Additionally, genes involved in the response to stress, such as the 2-component system response regulator *SRR1* and the carbonic anhydrase *NCE103*, are induced as well (Supplementary Table 4). Overall, this reaction is reminiscent of *C. albicans* encountering macrophages [33], confirming that the pathogen experiences antimicrobial stress in the dermis of CD4⁺ T cell–supplemented skin models.

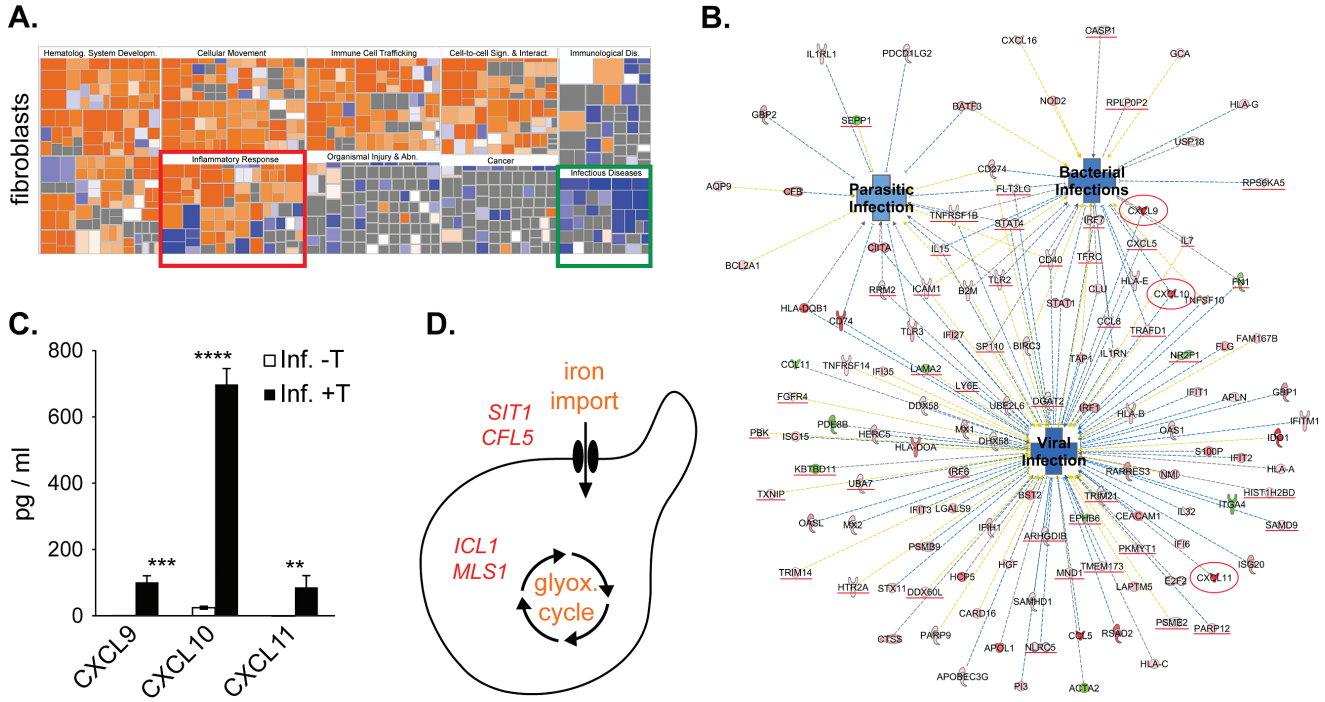

Figure 3. Differential expression analysis of fibroblasts and *Candida albicans* during invasion of T cell–supplemented skin models. *A*, Ingenuity pathway analysis (IPA) of differentially expressed genes (DEGs) in fibroblasts of infected skin models with or without CD4⁺ T cells. The heat map shows the *z* score of upregulated (orange) and downregulated (blue) cellular functions and diseases in the presence of CD4⁺ T cells. Threshold: average average log2 fold change (log2FC) of biological triplicates < –1.5 or > 1.5. Functions related to infectious diseases and an inflammatory response are highlighted by a green and red box, respectively. *B*, Gene networks predicted to reduce infectious diseases based on IPA. Up- and downregulated genes are colored in red and green, respectively. Predicted downregulated functions are shown in blue. Blue lines show consistent connections, and yellow lines show connections not supporting the IPA prediction. Gray lines show connections with unpredictable outcome. Threshold: average log2FC of biological triplicates < –1 or > 1, and genes with log2FC < –1.5 or > 1.5 are underlined. *C*, Quantification of CXCL9, CXCL10, and CXCL11 in the culture medium of infected skin models in the absence or presence of CD4⁺ T cells by enzyme-linked immunosorbent assay. Bars represent the mean and standard deviation of 3 independent skin models. Significant differences (2-tailed student *t* test): ** ($P < .01$), *** ($P < .001$), and **** ($P < .0001$). *D*, Differential expression analysis of *C. albicans* genes of fungi present in the dermis of skin models with or without CD4⁺ T cells. Significantly upregulated functions in the presence of T cells based on GO-term enrichment analysis are colored in orange, and upregulated genes belonging to these functions are shown in red. Threshold: average log2FC < –1 or > 1 and log2CPM > 1.5. Abbreviations: GO, gene ontology; Inf, infected; T, T cell.

Role of Toll-like Receptor 2 in Fibroblast Activation

Interleukin 17 and interleukin 22 (IL-22) produced by Th17 cells have previously been shown to be critically involved in epithelial defense against *C. albicans* invasion [34, 35], and genetic deficiencies in IL-17 signaling have been found in patients with chronic mucocutaneous candidiasis [36]. Addition of either IL-17A or IL-22 to skin models without $CD4^+$ T cells did, however, not result in significant dermal protection (Supplementary Figure 3A). Blocking of IL-17RA partially reverted $CD4^+$ T cell–mediated protection of skin models (Supplementary Figure 3B) but had no effect on induction of CXCL9, CXCL10, and CXCL11 in the presence of $CD4^+$ T cells as shown by ELISA (Supplementary Figure 3C). To identify the signaling pathways that lead to fibroblast reprogramming toward an antimicrobial phenotype, potential upstream regulatory networks were analyzed by IPA. This analysis revealed that, besides TNF- and interferon-signaling pathways, activation of Toll-like receptors (TLRs) or interleukin 1 receptors (IL1Rs) and subsequent NF-κB–dependent gene expression were most likely responsible for the observed changes (Figure 4A). Because NF-κB activation through TLRs and IL-1Rs is dependent on the protein kinase Irak4 [16, 37], we tested whether dermal protection is inefficient with fibroblasts from an Irak4-deficient patient [16]. As shown in Figure 4B, integration of Irak4-deficient fibroblasts into skin models resulted in a loss of protection against *C. albicans* invasion, showing that TLR/IL1R signal transduction is critical for this function. Toll-like receptor 2 was the most highly expressed TLR in dermal fibroblasts and upregulated during infection in the presence of $CD4^+$ T cells at the RNA level (Figure 4C), and its expression in fibroblasts in the dermal compartment could be confirmed by immunostaining (Figure 4D). Moreover, polymorphisms in this receptor have been associated previously with increased susceptibility to recurrent vulvovaginal candidiasis [4]. *o*-Vanillin has been shown recently to specifically inhibit TLR2 signaling [38], and using TLR2/TLR1 and TLR2/TLR6 expressing NIH3T3 reporter cells for NF-κB activation [18], we could confirm concentration-dependent inhibition of the signal activated through the synthetic TLR2 ligand Pam_3CysSK_4 (Figure 5A). As shown in Figure 5B and Supplementary Figure 3D, inhibition of TLR2 signaling by *o*-vanillin or knock

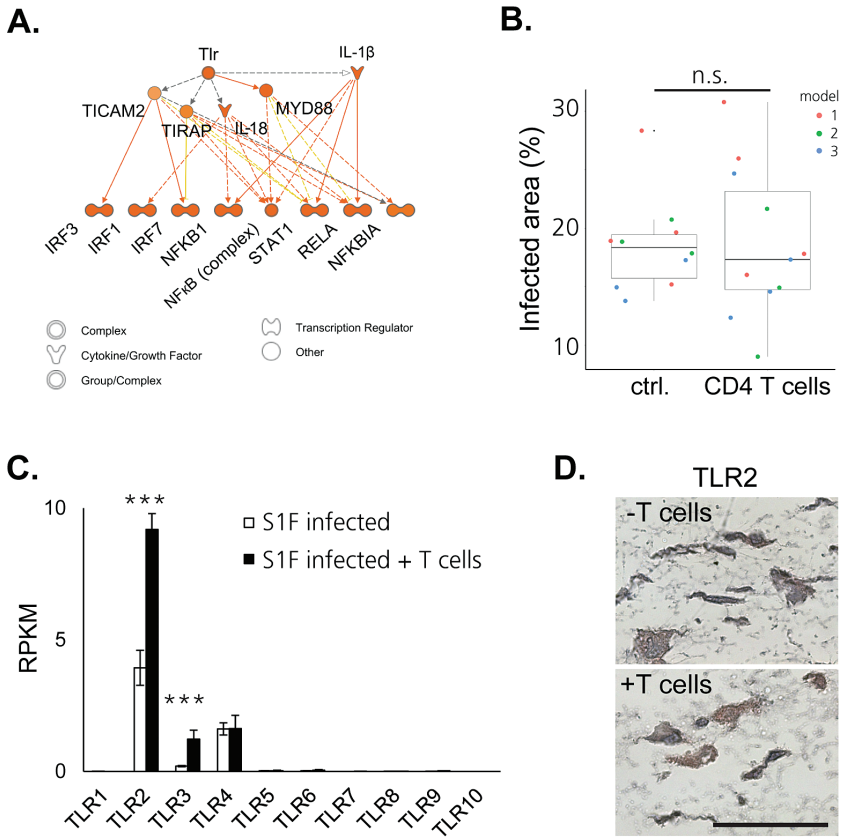

Figure 4. Role of NF-κB signaling in dermal protection against *Candida albicans* invasion. *A,* Prediction of upstream regulatory networks of expressional changes in fibroblasts from infected skin models in the presence or absence of $CD4^+$ T cells by Ingenuity pathway analysis. Molecules with predicted increased activity in the presence of T cells are highlighted in orange. *B,* Quantification of *C. albicans* dermal invasion of skin models with *Irak4*-deficient fibroblasts in the presence or absence of $CD4^+$ T cells 48 hours after infection. Statistical significance (2-tailed Wilcoxon-Mann-Whitney *U* test) in *A* and *B*: n.s. ($P > .05$). *C,* Expression levels of Toll-like receptor (TLR) genes in fibroblasts from skin models under different conditions as determined by RNA sequencing. Significant gene expression changes are indicated as *** (FDR < 0.001). *D,* Immunostaining of skin models with or without T cells, infected with *C. albicans* for 48 hours, for TLR2 expression (red) by dermal fibroblasts. Tissue sections were counterstained with Hemalaum (blue). Bar: 50 μm. Abbreviations: FDR, false discovery rate; n.s., not significant; RPKM, reads per kilobase per million mapped reads; TLR, Toll-like receptor.

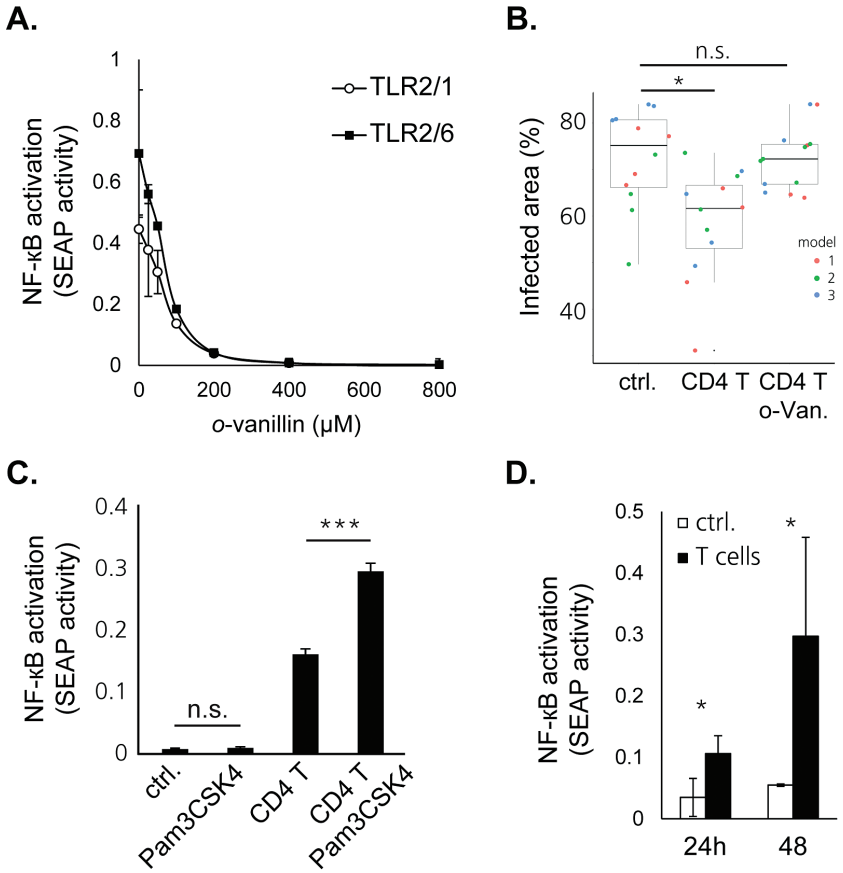

Figure 5. Role of Toll-like receptor 2 (TLR2) signaling in dermal protection against *Candida albicans* invasion. *A*, Reporter gene assay for NF-κB activation in response to Pam_3CysSK_4 and *o*-vanillin. NIH3T3 cells expressing secreted alkaline phosphatase (SEAP) under the control of an NF-κB promoter as well as TLR2 and Toll-like receptor 1 or TLR2 and Toll-like receptor 6 constitutively were treated with 1 ng/mL of the synthetic TLR2 agonist Pam_3CysSK_4 and different concentrations of *o*-vanillin for 24 hours, and SEAP activity was measured in the supernatant. The average and standard deviation of SEAP activity (A_{405nm}) of triplicate samples from a representative experiment out of 2 are shown. The A_{405nm} of *o*-vanillin alone was subtracted from each value. *B,* Quantification of *C. albicans* dermal invasion of skin models 48 hours after infection in the presence or absence of $CD4^+$ T cells and additional treatment with 200 μM *o*-vanillin for TLR2 signaling inhibition. Statistical significance (2-tailed Wilcoxon-Mann-Whitney *U* test): * ($P < .05$) and n.s. ($P > .05$). *C,* Reporter gene assay for NF-κB activation in fibroblasts. S1F fibroblasts expressing secreted alkaline phosphatase (S1F-SEAP) under the control of an NF-κB promoter were treated with 250 ng/mL of the synthetic TLR2 agonist Pam_3CysSK_4, 10^5 $CD4^+$ T cells, or a combination of both for 24 hours, and SEAP activity was measured in the supernatant. Bars show the average and standard deviation of SEAP activity of triplicate samples from a representative experiment out of 3. *D,* SEAP activity measured in the supernatants of skin models containing S1F-SEAP with or without $CD4^+$ T cells and *C. albicans* infection. The average and standard deviation of 3 skin models per group are shown. Significant differences (2-tailed student *t* test) in *C* and *D*: * ($P < .05$) and *** ($P < .001$). Abbreviations: n.s., not significant; SEAP, secreted alkaline phosphatase.

down of the receptor in fibroblasts reverted the protective effect observed in the presence of T cells. This confirms that the pathogen-derived signal leading to dermal protection by fibroblasts is mediated by TLR2. Toll-like receptor 2 activation alone was, however, not sufficient to drive NF-κB–dependent gene expression by dermal fibroblasts, as shown by Pam_3CysSK_4 treatment of fibroblasts expressing SEAP under the control of NF-κB (Figure 5C). Instead, Pam_3CysSK_4 was able to potentiate $CD4^+$ T cell–dependent NF-κB activation in dermal fibroblasts (Figure 5C). NF-κB reporter fibroblasts were also used for skin model construction to follow NF-κB–dependent gene expression during *C. albicans* infection. *Candida albicans* alone was an inefficient stimulus, whereas in the presence of $CD4^+$ T cells, fungal invasion resulted in a strong response of NF-κB reporter gene expression (Figure 5D). Together these results show that activation of dermal fibroblasts during *C. albicans* invasion requires signal transduction by TLR2 in combination with a second, $CD4^+$ T cell–derived signal.

$CD4^+$ T Cell Mediated Cleavage of Pro–Interleukin 1β

NF-κB may further be activated in an Irak-4-dependent manner by the proinflammatory interleukin IL-1β. Using reporter gene assays, we could see that IL-1β was able to activate NF-κB–dependent SEAP expression in dermal fibroblasts (Figure 6A). Moreover, addition of IL-1β to 3D skin models significantly reduced dermal *C. albicans* invasion in a manner similar to $CD4^+$ T cells (Figure 6B). Interleukin 1β was already induced during skin model invasion in the absence of T cells, as seen by RNA sequencing (Figure 6C). By Western blot, however, we could see that only inactive pro–IL-1β was expressed in

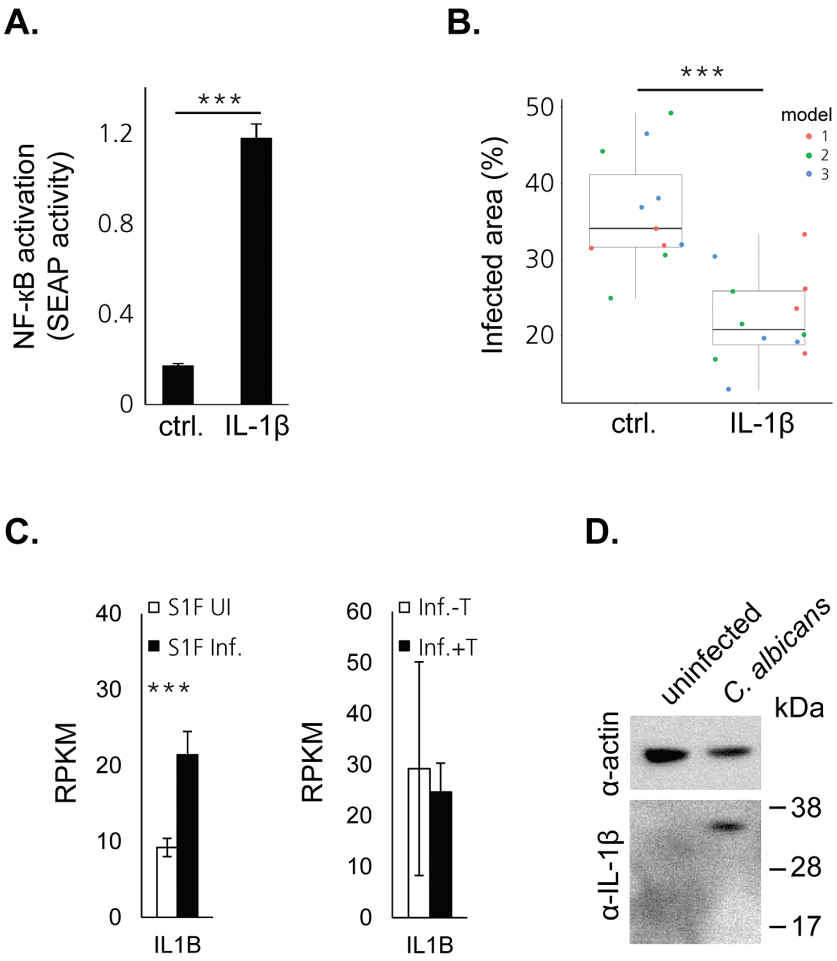

Figure 6. Role of interleukin 1β (IL-1β) in dermal protection against *Candida albicans* invasion. *A,* S1F fibroblasts expressing secreted alkaline phosphatase (S1F-SEAP) cells were treated with 200 pg/mL IL-1β for 48 hours, and SEAP activity was measured in the supernatant. Bars show the average and standard deviation of SEAP activity of 6 samples from 1 representative experiment out of 3. Significant differences (2-tailed student *t* test): *** ($P < .001$). *B,* Depth of dermal *C. albicans* invasion 48 hours after infection of skin models treated with 200 pg/mL of IL-1β. Significant differences (2-tailed Wilcoxon-Mann-Whitney *U* test): *** ($P < .001$). *C,* Interleukin 1β expression levels in fibroblasts from skin models under different conditions as determined by RNA sequencing. Significant gene expression changes: *** (FDR < 0.001). *D,* Pro–IL-1β expression in uninfected or infected S1F fibroblasts 48 hours after infection as determined by Western blot of cell lysates. Actin was used as a loading control. Abbreviations: *C. albicans*, *Candida albicans*; FDR, false discovery rate; IL-1β, interleukin 1β; Inf, infected; RPKM, reads per kilobase per million mapped reads; SEAP, secreted alkaline phosphatase; T, T cell; UI, uninfected.

fibroblasts in the presence of *C. albicans* alone; active cleaved IL-1β was not detected in the cells by Western blot as a band at 17 kDa, and secreted IL-1β was not found in the supernatant by ELISA (Figure 6D and Figure 7A). Interleukin 1β expression is known to be induced in response to TLR activation [39], but for proteolytic cleavage by caspase-1, additional activation of the inflammasome through a danger signal such as membrane damage is required [39, 40]. During *C. albicans* infection of skin models, neither the conventional nor the nonconventional NLRP3 inflammasome or alternative inflammasome components were upregulated, even in the presence of $CD4^+$ T cells (Figure 7B; Supplementary Figure 3E). Moreover, by immunostaining ASC could be detected in keratinocytes, predominantly in the apical part of the epidermis, but not in dermal fibroblasts under these conditions (Figure 7C). Nevertheless, the presence of T cells promoted induction and activation of caspase-1 (Figure 7B and 7D) as well as secretion of IL-1β during infection by dermal fibroblasts (Figure 7A). In conclusion, *C. albicans* dermal invasion alone is insufficient to promote inflammasome-dependent IL-1β processing and full activation of IL-1β–dependent transcriptional changes through NF-κB. However, in the presence of $CD4^+$ T cells, IL-1β induced in response to *C. albicans* is cleaved and secreted. This results in full activation of fibroblasts and reprogramming toward an antimicrobial phenotype (Supplementary Figure 4).

DISCUSSION

In this study we used a $CD4^+$ T cell–supplemented human skin model to identify intercellular communication mechanisms that result in dermal protection against *C. albicans* invasion. This in vitro cell-culture model is structurally similar to natural human skin, containing a stratified and cornified epidermis and

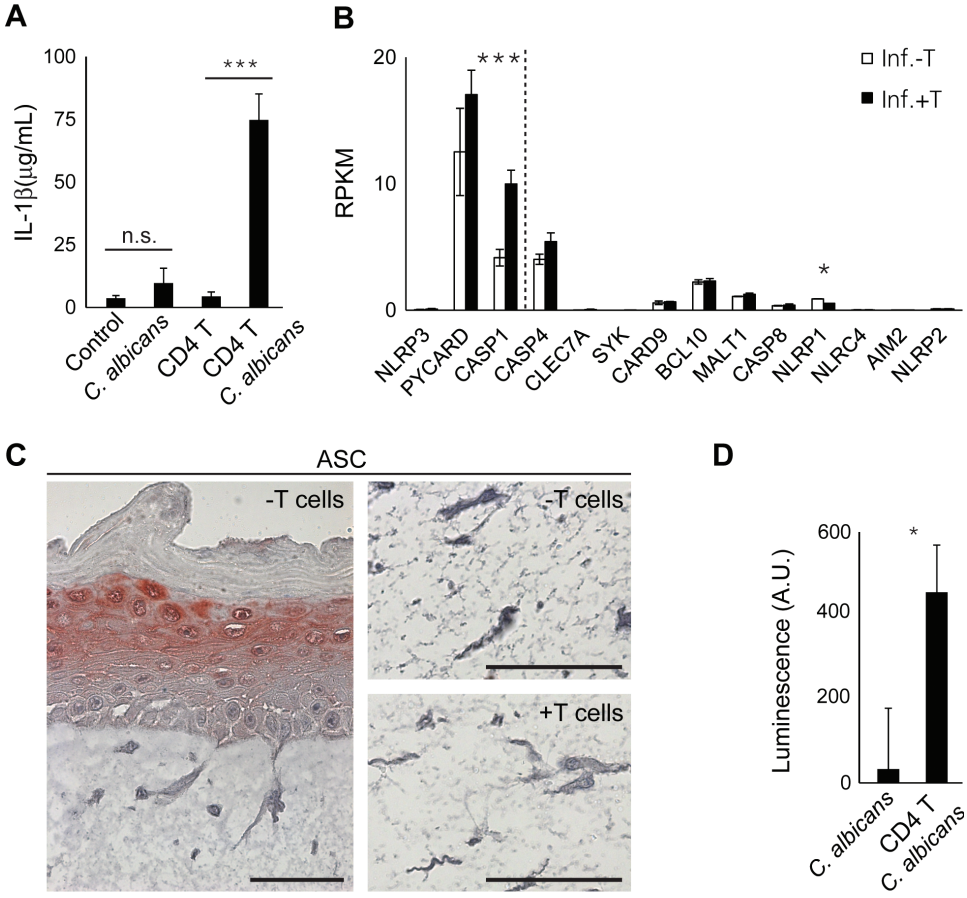

Figure 7. Expression and secretion of interleukin 1β (IL-1β) by dermal fibroblasts. *A*, Detection of IL-1β by enzyme-linked immunosorbent assay in the supernatant of S1F alone or cocultured with CD4+ T cells and infected with *Candida albicans* for 48 hours. *B*, Expression levels of inflammasome-related genes in fibroblasts from infected skin models with or without CD4+ T cells as determined by RNA sequencing. Significant gene expression changes: * (FDR < 0.05), *** (FDR < 0.001). The Mean and standard deviation of triplicates are shown. *C*, Immunostaining for ASC (red) of skin models with or without T cells and infected for 48 hours with *C. albicans*. An intact noncolonized epidermal area (left) and dermal areas (right) are shown. Sections were counterstained with Hemalaum. Bars: 50 μm. *D*, Measurement of caspase-1 activity in culture supernatant from skin models with or without T cells and infected with *C. albicans* for 48 hours. Bars represent the mean and standard deviation of 3 independent tissue models. Significant differences (2-tailed student *t* test) in *A* and *D*: * ($P < .05$) and *** ($P < .001$). Abbreviations: ASC, apoptosis-associated speck-like protein containing CARD; *C. albicans*, *Candida albicans*; FDR, false discovery rate; IL-1β, interleukin 1β; Inf, infected; RPKM, reads per kilobase per million mapped reads; T, T cell.

a dermal compartment with fibroblasts embedded in collagenous extracellular matrix. Moreover, gene expression patterns of various epidermal differentiation markers are identical to natural skin, and general expression profiles of keratinocytes and dermal fibroblasts resemble previously described expression profiles of these skin cell types. Nevertheless, various skin structures, including hair follicles, sweat glands, and blood vessels, as well as diverse cell types, such as melanocytes, neuronal cells, and Langerhans cells, among others, are not present in this model. We aim to add some of these components in the future. Several cell types, including neutrophils, Th17 cells, γδ T cells, and epithelial cells themselves, are already known to be involved in epithelial protection against fungal invasion [2, 6–9]. The reduced system, which contained only keratinocytes, fibroblasts, and CD4+ T cells that can be manipulated and analyzed separately, allowed us to identify additional routes of communication between a minimal set of cells and *C. albicans* that result in subepithelial, dermal protection against fungal invasion.

We found that TLR2 expression and activation in fibroblasts is required but not sufficient for protection. In keratinocytes, it was shown that TLR2 signaling, induced by *C. albicans*–derived phospholipomannan, is sufficient to trigger an antimicrobial response [9]. In dermal fibroblasts, we found in contrast that a second signal, which induces secretion of cleaved IL-1β by these cells, is also necessary. Interleukin 1β expression was induced in dermal fibroblasts upon infection. It was, however, secreted only in the presence of CD4+ T cells. Notably, ASC was not detected by immunostaining in fibroblasts, and by expressional profiling we did not observe induction of inflammasome-related genes that could explain caspase-1 activation and subsequent proteolytic cleavage and release of IL-1β. Caspase-1 may therefore be activated by an alternative mechanism—for example, through TNF-α signaling, as recently shown in adipocytes [41], or by

the interferon-inducible GBP2, as demonstrated in the context of bacterial infection [32, 42]. Interestingly, GBP2 is among the significantly upregulated genes in fibroblasts during *C. albicans* infection in the presence of $CD4^+$ T cells.

We have also tested for a role of IL-17 or IL-22 in $CD4^+$ T cell–dependent dermal protection of skin models by addition of recombinant proteins or an IL-17RA blocking antibody. Because we did not see a decisive influence on dermal protection of this in vitro, we conclude that these cytokines, which play a critical role in first-line epithelial defense, are not primarily responsible for the protection of the subepithelial compartment, as has been reviewed earlier [2]. Deciphering the T cell–derived signal that results in IL-1β secretion by fibroblasts and the stimulation of an antimicrobial response will be a focus in the future.

The expression pattern of the fibroblast-derived antimicrobial response was remarkably broad, indicating that it may act against diverse classes of pathogens. In this line, induction of antiviral genes in dermal fibroblasts was found recently during infection with Zikavirus, Chikunguniavirus, and West Nile virus [43–45].

Besides the direct antimicrobial response, we could also observe upregulation of functions, such as antigen presentation and chemotaxis of diverse cell types in fibroblasts, in response to *C. albicans* and $CD4^+$ T cells, indicating that these cells can shape the global immune response to the invading pathogen. Altogether the results presented here show that dermal fibroblasts may play a yet unappreciated central role in pathogen defense by integrating signals from the microenvironment in subepithelial tissue. This potentially opens new possibilities for host-targeted anti-infective therapies based on immunomodulation of fibroblasts.

Supplementary Data

Supplementary materials are available at *The Journal of Infectious Diseases* online. Consisting of data provided by the authors to benefit the reader, the posted materials are not copyedited and are the sole responsibility of the authors, so questions or comments should be addressed to the corresponding author.

Notes

Acknowledgments. The authors thank Leif Schauser and Nitesh Kumar Singh for introduction into Ingenuity pathway analysis. The authors would also like to thank Anne Puel for providing IRAK4-deficient human dermal fibroblasts.

Financial support. This work was supported by a fellowship to A. K. within the FP7-PEOPLE-2013-ITN - Marie-Curie Action: "Initial Training Networks," (Project ID: 606786) and by the Fraunhofer Gesellschaft.

Potential conflicts of interest. All authors: No reported conflicts of interest. All authors have submitted the ICMJE Form for Disclosure of Potential Conflicts of Interest. Conflicts that the editors consider relevant to the content of the manuscript have been disclosed.

References

1. Fidel PL Jr. Distinct protective host defenses against oral and vaginal candidiasis. Med Mycol **2002**; 40:359–75.
2. Kashem SW, Kaplan DH. Skin immunity to *Candida albicans*. Trends Immunol **2016**; 37:440–50.
3. Smeekens SP, van de Veerdonk FL, Kullberg BJ, Netea MG. Genetic susceptibility to *Candida* infections. EMBO Mol Med **2013**; 5:805–13.
4. Rosentul DC, Delsing CE, Jaeger M, et al. Gene polymorphisms in pattern recognition receptors and susceptibility to idiopathic recurrent vulvovaginal candidiasis. Front Microbiol **2014**; 5:483.
5. Maródi L, Cypowyj S, Tóth B, Chernyshova L, Puel A, Casanova JL. Molecular mechanisms of mucocutaneous immunity against *Candida* and *Staphylococcus* species. J Allergy Clin Immunol **2012**; 130:1019–27.
6. Weindl G, Naglik JR, Kaesler S, et al. Human epithelial cells establish direct antifungal defense through TLR4-mediated signaling. J Clin Invest **2007**; 117:3664–72.
7. Trautwein-Weidner K, Gladiator A, Nur S, Diethelm P, LeibundGut-Landmann S. IL-17-mediated antifungal defense in the oral mucosa is independent of neutrophils. Mucosal Immunol **2015**; 8:221–31.
8. Naglik JR, Richardson JP, Moyes DL. Candida albicans pathogenicity and epithelial immunity. PLoS Pathog **2014**; 10:e1004257.
9. Li M, Chen Q, Tang R, Shen Y, Liu WD. The expression of β-defensin-2, 3 and LL-37 induced by *Candida albicans* phospholipomannan in human keratinocytes. J Dermatol Sci **2011**; 61:72–5.
10. Naglik JR, Moyes DL, Wächtler B, Hube B. *Candida albicans* interactions with epithelial cells and mucosal immunity. Microbes Infect **2011**; 13:963–76.
11. Perlroth J, Choi B, Spellberg B. Nosocomial fungal infections: epidemiology, diagnosis, and treatment. Med Mycol **2007**; 45:321–46.
12. Nucci M, Anaissie E. Revisiting the source of candidemia: skin or gut? Clin Infect Dis **2001**; 33:1959–67.
13. Kashem SW, Igyártó BZ, Gerami-Nejad M, et al. *Candida albicans* morphology and dendritic cell subsets determine T helper cell differentiation. Immunity **2015**; 42:356–66.
14. Dickson MA, Hahn WC, Ino Y, et al. Human keratinocytes that express hTERT and also bypass a p16(INK4a)-enforced mechanism that limits life span become immortal yet retain normal growth and differentiation characteristics. Mol Cell Biol **2000**; 20:1436–47.
15. Rheinwald JG, Hahn WC, Ramsey MR, et al. A two-stage, p16(INK4A)- and p53-dependent keratinocyte senescence mechanism that limits replicative potential independent of telomere status. Mol Cell Biol **2002**; 22:5157–72.
16. Davidson DJ, Currie AJ, Bowdish DM, et al. IRAK-4 mutation (Q293X): rapid detection and characterization of defective post-transcriptional TLR/IL-1R responses in human myeloid and non-myeloid cells. J Immunol **2006**; 177:8202–11.
17. Ramirez RD, Herbert BS, Vaughan MB, et al. Bypass of telomere-dependent replicative senescence (M1) upon overexpression of Cdk4 in normal human epithelial cells. Oncogene **2003**; 22:433–44.
18. Burger-Kentischer A, Abele IS, Finkelmeier D, Wiesmüller KH, Rupp S. A new cell-based innate immune receptor assay for the examination of receptor activity, ligand specificity, signalling pathways and the detection of pyrogens. J Immunol Methods **2010**; 358:93–103.
19. Gillum AM, Tsay EY, Kirsch DR. Isolation of the *Candida albicans* gene for orotidine-5'-phosphate decarboxylase by complementation of *S. cerevisiae* ura3 and *E. coli* pyrF mutations. Mol Gen Genet **1984**; 198:179–82.
20. Kühbacher A, Sohn K, Burger-Kentischer A, Rupp S. Immune cell-supplemented human skin model for studying fungal infections. Methods Mol Biol **2017**; 1508:439–49.
21. Hernandez R, Rupp S. Human epithelial model systems for the study of *Candida* infections in vitro: part II. Histologic methods for studying fungal invasion. Methods Mol Biol **2009**; 470:105–23.
22. Schneider CA, Rasband WS, Eliceiri KW. NIH Image to ImageJ: 25 years of image analysis. Nat Methods **2012**; 9:671–5.
23. Edgar R, Domrachev M, Lash AE. Gene Expression Omnibus: NCBI gene expression and hybridization array data repository. Nucleic Acids Res **2002**; 30:207–10.
24. Citiulo F, Jacobsen ID, Miramón P, et al. Candida albicans scavenges host zinc via Pra1 during endothelial invasion. PLoS Pathog **2012**; 8:e1002777.
25. Cole AM, Ganz T, Liese AM, Burdick MD, Liu L, Strieter RM. Cutting edge: IFN-inducible ELR-CXC chemokines display defensin-like antimicrobial activity. J Immunol **2001**; 167:623–7.
26. Holdren GO, Rosenthal DJ, Yang J, et al. Antimicrobial activity of chemokine CXCL10 for dermal and oral microorganisms. Antibiotics (Basel) **2014**; 3:527–39.
27. Yung SC, Murphy PM. Antimicrobial chemokines. Front Immunol **2012**; 3:276.
28. Krishnakumari V, Rangaraj N, Nagaraj R. Antifungal activities of human beta-defensins HBD-1 to HBD-3 and their C-terminal analogs Phd1 to Phd3. Antimicrob Agents Chemother **2009**; 53:256–60.
29. Schröder JM, Harder J. Human beta-defensin-2. Int J Biochem Cell Biol **1999**; 31:645–51.
30. Al-Zeer MA, Al-Younes HM, Lauster D, Abu Lubad M, Meyer TF. Autophagy restricts *Chlamydia trachomatis* growth in human macrophages via IFNG-inducible guanylate binding proteins. Autophagy **2013**; 9:50–62.

31. Degrandi D, Kravets E, Konermann C, et al. Murine guanylate binding protein 2 (mGBP2) controls *Toxoplasma gondii* replication. Proc Natl Acad Sci U S A **2013**; 110:294–9.
32. Meunier E, Wallet P, Dreier RF, et al. Guanylate-binding proteins promote activation of the AIM2 inflammasome during infection with *Francisella novicida*. Nat Immunol **2015**; 16:476–84.
33. Lorenz MC, Bender JA, Fink GR. Transcriptional response of *Candida albicans* upon internalization by macrophages. Eukaryot Cell **2004**; 3:1076–87.
34. De Luca A, Zelante T, D'Angelo C, et al. IL-22 defines a novel immune pathway of antifungal resistance. Mucosal Immunol **2010**; 3:361–73.
35. Conti HR, Shen F, Nayyar N, et al. Th17 cells and IL-17 receptor signaling are essential for mucosal host defense against oral candidiasis. J Exp Med **2009**; 206:299–311.
36. Puel A, Cypowyj S, Bustamante J, et al. Chronic mucocutaneous candidiasis in humans with inborn errors of interleukin-17 immunity. Science **2011**; 332:65–8.
37. Verstrepen L, Bekaert T, Chau TL, Tavernier J, Chariot A, Beyaert R. TLR-4, IL-1R and TNF-R signaling to NF-kappaB: variations on a common theme. Cell Mol Life Sci **2008**; 65:2964–78.
38. Mistry P, Laird MH, Schwarz RS, et al. Inhibition of TLR2 signaling by small molecule inhibitors targeting a pocket within the TLR2 TIR domain. Proc Natl Acad Sci U S A **2015**; 112:5455–60.
39. Netea MG, van de Veerdonk FL, Kullberg BJ, Van der Meer JW, Joosten LA. The role of NLRs and TLRs in the activation of the inflammasome. Expert Opin Biol Ther **2008**; 8:1867–72.
40. Sharma D, Kanneganti TD. The cell biology of inflammasomes: mechanisms of inflammasome activation and regulation. J Cell Biol **2016**; 213:617–29.
41. Furuoka M, Ozaki K, Sadatomi D, et al. TNF-α induces caspase-1 activation independently of simultaneously induced NLRP3 in 3T3-L1 cells. J Cell Physiol **2016**; 231:2761–7.
42. Finethy R, Jorgensen I, Haldar AK, et al. Guanylate binding proteins enable rapid activation of canonical and noncanonical inflammasomes in *Chlamydia*-infected macrophages. Infect Immun **2015**; 83:4740–9.
43. Ekchariyawat P, Hamel R, Bernard E, et al. Inflammasome signaling pathways exert antiviral effect against Chikungunya virus in human dermal fibroblasts. Infect Genet Evol **2015**; 32:401–8.
44. Hamel R, Dejarnac O, Wichit S, et al. Biology of Zika virus infection in human skin cells. J Virol **2015**; 89:8880–96.
45. Hoover LI, Fredericksen BL. IFN-dependent and -independent reduction in West Nile virus infectivity in human dermal fibroblasts. Viruses **2014**; 6:1424–41.